Virginia Journal of Science
Volume 71, Issue 1 & 2
Spring & Summer 2020
doi: 10.25778/ghvj-gb62

Note: This manuscript has been accepted for publication and is online ahead of print. It will undergo copyediting, typesetting, and review of the resulting proof before it is published in its final form.

Assessing Microplastic Pollution in Four Mile Run, an Urban Stream in Northern Virginia

Kurt Moser[1], Tessa Naughton-Rockwell[2], Louisa Wang[3], Ethan Litmans[3], and Amanda Manoogian[4]

[1] Four Mile Run Conservatory Foundation
[2] Virginia Polytechnic Institute and State University
[3] Georgetown Day School
[4] Middlebury College

ABSTRACT

Microplastics are pollutants of concern in waterways and oceans for their persistence and impact on aquatic life and food webs. This study demonstrates a low-cost land-based sampling method to assess the extent of microplastic pollution found in Four Mile Run, an urban stream in Northern Virginia. Microplastic particle counts in environmental and treated wastewater ranged from 0.01-0.24 particles L^{-1} (mean 0.08 particles L^{-1}) and from 2 to 446 μg L^{-1} (mean 70 μg L^{-1}), with fibers found to be the most common microplastic category. Treated wastewater effluent was found to be a significant source of microplastic pollution, though microplastics were also found upstream of any influence from wastewater or tide-borne materials. The sampling method proved effective for collecting and analyzing microplastic pollution, though the sample size of 100 L was deemed insufficient for reliable measurement of total mass of microplastics.

Keywords: Microplastic, Pollution, Urban, Water

INTRODUCTION

Plastic has been an important material for humankind in the last century, and it is ubiquitous in daily life. Often used for packaging and other single-use applications, plastic is an inexpensive material with favorable properties such as strength, light weight, durability, and water resistance. Rather than breaking down chemically when weathered, plastic items (e.g., litter) break apart into smaller and smaller fragments, persisting in the environment. While there is no scientific standard for the size at which such fragments are designated microplastics, many authors have adopted an upper size threshhold of 5 mm, with particles smaller than 100 nm considered nanoplastics (Koelmans et al. 2019, Prata 2018, Horton et al. 2017, Koelmans et al 2015, Masura et al. 2015). Microplastics are *primary microplastics* when they originate in the size class, as is the case with virgin plastic

pellets used as raw material in manufacturing, and with so-called 'microbeads' used in cosmetic and abrasive products (Horton et al. 2017). *Secondary microplastics* are fragments derived from plastic products such as single-use plastic containers and bags (e.g., litter), broken plastic tools, toys, or household items, and fibers shed from synthetic fabrics, carpets, and other textiles (Ibid).

Microplastics have received recent attention for their presence in natural environments, notably in areas of concentrated floating debris, as in subtropical gyres of the world's major oceans (Ryan 2015), but as a human-created product, plastics originate on land. When plastic and plastic waste are mismanaged they are often transported and weathered in freshwater systems prior to reaching the ocean. We thus expect streams and rivers to transport and contain microplastics, and there is a growing body of evidence to show it. Microplastics have been found in large freshwater lakes (Eriksen et al. 2013), river sediments (Castaneda et al. 2014), and in smaller water bodies, even ones far removed from human activity (Horton et al. 2017). They have also been found in drinking water and its sources (Koelmans et al. 2019).

With mounting concern over the widespread microplastic contamination of aquatic ecosystems, some studies have explored the effects and potential impact of microplastics on ecosystem and organism health, either through intrinsic chemical toxicity or as a vector for organic pollutants and heavy metals (Chae & An 2017). Microplastics are ingested by a variety of marine and freshwater organisms and incorporated into tissues, affecting feeding behavior, reproduction, viability, and mortality (Chae & An 2017, Herzke et al. 2016, Sussarellu et al. 2016, Tanaka & Takada 2016, Hall et al. 2015). In marine and freshwater studies, microplastics have been shown to absorb toxic pollutants readily (Nguyen et al. 2019, Chae & An 2017, Mato et al. 2001). Through bioaccumulation, microplastics and any associated toxins may concentrate higher up the food chain, potentially finding their way onto the plates of consumers (Smith et al. 2018, Rochman et al. 2015, Tanaka et al. 2013).

High concentrations of microplastics have been found in waterways in urban settings (Vermaire et al. 2017, Dris et al. 2015, McCormick et al. 2014, Moore et al. 2011), and microplastic loads to surface waters appear to increase with urban density (Rhoades et al. 2019, Baldwin et al. 2016, Yonkos 2014). In populated areas with sanitary sewer systems, treated wastewater can also be a source of microplastics, particularly fibers, to receiving waters, even though treatment systems are capable of removing a large proportion of microplastics borne in raw sewage (Le Tarte et al. 2019, Burns et al. 2018, Leslie et al. 2017, McCormick et al. 2016).

The present study examines microplastic pollution in Four Mile Run, a Potomac River tributary that flows through Arlington and Fairfax counties and the cities of Falls Church and Alexandria in northern Virginia, USA (Figure 1). The Four Mile Run watershed drains a highly urbanized area of 51 km^2, with estimates of impervious surface cover exceeding 35% (Davey Resource Group 2017, Fry et al. 2011). Four Mile Run's annual-mean discharge ranges from 0.23 to 1.16 $m^3 s^{-1}$ upstream of tidal influence (USGS 2019). During rainfall events, however, peak flows routinely exceed 90 $m^3 s^{-1}$, reflecting

its urban hydrology. With more than 200,000 people living in the watershed, human impacts are inevitable. Arlington County's wastewater treatment plant discharges treated water into the tidal channel at an average rate of 87,000 m^3 d^{-1}, or roughly 1 m^3 s^{-1} (Arlington County, 2019). The Virginia Department of Environmental Quality has listed Four Mile Run as impaired under section 303(d) of the Clean Water Act for bacteria and for PCB and chlordane contamination in fish tissue (Virginia DEQ 2018, NVRC 2004). The Run is also significantly impacted by litter. Each year volunteers with the Four Mile Run Conservatory Foundation remove more than two tons of litter, much of which is plastic. In seventeen years of Arlington community clean-ups upstream on the Run, three quarters of the litter items collected have been plastic, a third of which were in the form of plastic/foam fragments (EcoAction Arlington 2019).

The goal of the present study is to document the extent of microplastic pollution in Four Mile Run, describing the quantities and types of microplastics found, using a land-based method for sampling in urban streams that are too shallow for the use of conventional tow-net protocols. Our research questions include how the microplastic pollution compares to that found in other freshwater settings and what types or sources of microplastics can be found. Four Mile Run is an outlier among the kinds of freshwater streams that have been studied: it is one of the smallest in terms of watershed area and discharge, yet possibly the highest in population density, compared to tidal and non-tidal waterways in existing studies covering more than 50 freshwater rivers and streams (Rhoades et al. 2019, Horton et al. 2017, Vermaire et al. 2017, Baldwin et al. 2016, McCormick et al. 2016, Dris et al. 2015, McCormick et al. 2014, Yonkos 2014, Moore et al. 2011). Because so few studies have examined freshwater streams of Four Mile Run's small size or extent of urbanization, the results of this study can inform future research, particularly studies that could be conducted by volunteers or nonprofit groups using inexpensive equipment and analytical techniques suited to a school chemistry lab or comparable small facility.

METHODS

Sampling was conducted in June 2018 and in May/June 2019 during the course of the Four Mile Run Conservatory Foundation's summer intern field season, as schedule, weather, and safety conditions allowed. Water samples were collected from locations at lower Four Mile Run in the City of Alexandria and Arlington County, Virginia (Figure 2). Sample locations were all within a 1 km radius of the Mount Vernon Avenue bridge, ranging from tidal to non-tidal waters within the flood control levee system. Samples were collected from four general locations: on upstream non-tidal main stem and tributary waters above the confluence of Lower Long Branch Creek (UP); near the head of tide on the main stem of Four Mile Run near the Mount Vernon Avenue bridge (FM); at the Hume Spring tributary mouth and at the large stormwater outfall near its head (HS); and from treated wastewater effluent at the Arlington Water Pollution Control Plant outfall (TP).

With modifications noted below, the methods used in this study follow the procedures outlined by the National Oceanic and Atmospheric Administration for microplastic sampling and analysis (Masura et al. 2015). Precautions were taken at every stage of sample collection, handling, processing, and analysis to avoid and minimize microplastic contamination of samples, though it would be impractical to eliminate every

potential microplastic contaminant source. Non-plastic materials were used as much as possible, and where plastic equipment was considered necessary, it was inspected to ensure it was in good condition, without apparent wear or likelihood of material loss. Specific precautions are additionally described below. Equipment/materials made of plastic or with plastic components included: sample jar caps/liners, rinse bottles, spray bottle, bungee cords, portable field table, equipment transport buckets, hip waders, eyeglasses, safety goggles, lab smocks and gloves, reagent bottles, digital thermometers, magnetic stir bars, custom sieves, vial caps, and microscopes.

Field protocol

Precautions taken to avoid microplastic contamination during sample collection included wearing non-synthetic clothing while sampling, rinsing the sample collection bucket with stream water several times at each sampling site, collecting samples up-current of where the researcher and field equipment were located, applying rinse water (tap water) only from the reverse side of the sieve, and using new, clean glass sample jars. At each sampling site, equipment was checked to ensure it was free of extraneous material and in good condition.

Water samples were collected by repeated draws of a galvanized steel bucket which had been modified so that twelve draws of the bucket resulted in 100 L of water sampled. The sample volume was arbitrarily selected as practical for land-based hand sampling, while sufficiently large to ensure a measurable amount of solid material after sieve filtration. Modification of the bucket, of approximately 10 L nominal size, consisted of filling it with 8.33 L measured volume of tap water, marking the water level while the bucket was lifted/supported by its handle, then drilling holes on one side at and above the marked water line, so that sample water could be poured from the opposite side in a controlled manner. Samples were reduced in volume by sieve filtration, pouring from the bucket through two stacked sieves, the upper sieve a #3.5 mesh stainless steel test sieve, allowing only materials of size approximately 5 mm or less to pass through, and the lower sieve a #50 mesh brass test sieve, retaining particles larger than 300 µm. As in microplastic studies that commonly use towed neuston nets, materials in the microplastic size range of 300 µm to 5 mm were thus retained from the lower sieve. All other materials were discarded. Sieved materials were transferred from the lower sieve into 240-mL glass sample collection jars by careful rinsing with tap water filled rinse bottles from the reverse side of the sieve, with material scraped with a metal scoopula and/or bamboo scraper where needed, until no microplastic or other materials were visible in the sieve. Each finished sample consisted of solid materials in approximately 40-100 mL of rinse water.

Laboratory protocol

Field-collected samples were analyzed using the procedure outlined in NOAA guidance for microplastic analysis of water samples (Masura et al. 2015) by wet peroxide oxidation/digestion, without the iron catalyst (Figure 3). We chose not to use the catalyst because we believed it to be a simpler and safer procedure, suitable for volunteers, and because our samples contained far less material than is typical for tow-net collected samples. To minimize post-sampling contamination from indoor air, samples were kept covered with foil when not in use, and as much as practical, non-synthetic materials were

utilized, such as paper tape, foil, natural fiber clothing, and metal tools, with deionized water used for solutions and rinsing glassware. Glassware was washed and rinsed with deionized water immediately prior to use. Where plastic equipment was used during lab procedures, as with squirt bottles for rinsing samples and equipment, it was inspected visually to ensure it was in good condition and unlikely to be a source of contaminants.

The samples were transferred into clean pre-weighed 150-mL beakers, using a spatula and minimal rinsing with deionized water. The beakers were loosely covered with foil and samples then air-dried in drying ovens at 90-95°C for 24 hours or longer, to sample dryness, allowed to cool, and weighed for total mass of solids. In a fume hood, 20 mL of 30% hydrogen peroxide was added to each beaker. The beaker was allowed to stand at ambient temperature for at least five minutes before adding a stir bar and heating to 75°C on a hot plate. The temperature was then maintained at 75°C for at least 30 minutes, with 30% hydrogen peroxide added as needed to replenish evaporated liquid, and until much of the natural material (e.g., algae, leaf material) was no longer visible in the beaker. When oxidation/digestion was complete, approximately 6 g salt (NaCl) per 20 mL of sample was added to increase the density of the solution, before transferring the solution to a density separator, covering, and allowing it to settle for at least 24 hours. Settled solids (non-plastic) were drained, inspected, and discarded, with floating and suspended solids collected/rinsed onto a clean 300-µm custom sieve, covered with foil, and air-dried. The custom sieves were made from approximate 25-mm lengths of 52-mm inner-diameter PVC pipe (nominal 2-inch), to which 300-µm nylon mesh screening was affixed using a multi-material gel adhesive, as per Masura et al. 2015.

The 300-µm custom sieves were examined under a dissecting microscope. Microplastic items were visually discerned by color and/or shape, distinct from plant materials such as seed coats or plant fibers. Hard plastic materials were additionally discerned by their durability and resistance to light pressure from metal forceps, whereas natural materials tended to come apart easily. Plastic foam materials also resisted pressure, returning to form readily, whereas natural foam-like materials deformed or broke apart. Items identified as microplastics were removed from the sieve and transferred using forceps into a clean and pre-weighed 4-mL vial. Total mass of microplastics was then determined to the nearest 0.1 mg. Microplastic particles were counted and classified into five categories: pellet, fragment, fiber, film, and sponge/foam.

RESULTS

Microplastics were found in every sample, in spite of the small sample sizes (Table 1). Particle counts ranged from 1 to 24 microplastic particles per 100 L sample, with a median of 7 and mean of 8 particles per sample. The concentrations of microplastic materials ranged from 2 to 446 µg L^{-1}, with a median of 13 and a mean of 70 µg L^{-1}.

Fibers accounted for the majority of microplastic particles, followed by fragments and sponge/foam pieces (Figure 4). Although the method used would be expected to capture particles in sizes up to 5.6 mm, based on the mesh size, the microplastic particles recovered from the procedure were all sized 1 mm or less, though a few of the tangled fiber particles, if fully extended, would have been of length greater than 1 mm. No pellet-type

microplastics were found. The sites at which the samples were collected differed somewhat in their composition by microplastic category. For example, foam particles were a more prominent component of the tidal Hume Spring samples, though the nature of tidal influence could not be effectively determined, as the number of samples collected was insufficient for comparison, given the variety of tidal conditions (incoming/outgoing, various stages) during sampling.

Because some samples were collected within a day of localized rainfall, it was expected that they might contain higher concentrations of microplastics due to stormwater pollutants and re-suspension of stream sediments. The non-wastewater samples collected in 2019 were compared to determine whether they differed depending on whether or not they had been collected within 24 hours after rain events, as recorded at the USGS gage station 01652500 (USGS 2019), located 1.9 km upstream from the Mount Vernon Avenue bridge. Because the variances differed between the rain (n=5) and no-rain (n=5) groups, for both the number of microplastic particles and the masses of microplastics, the non-parametric Wilcoxon rank-sum test was used to compare the two groups. For both tests, the critical value for $\alpha = .05$ (two-tail) is $W_{crit} = 17$. Both tests resulted in $W = 24.5$, thus the null hypothesis is not rejected, and no significant difference was found.

DISCUSSION

Microplastics in Four Mile Run

Secondary microplastics, derived from the breakdown of larger plastic items, were evident in all Four Mile Run samples, while primary microplastics, associated with manufacturing (e.g., pellets) and cosmetics/abrasives (e.g., microbeads) were not found. Among the microplastic particles, fibers were the most prevalent category. They were present in 11 of 14 samples, from tidal and non-tidal sites and from wastewater effluent. This is consistent with the assessment that fibers are abundant and often prevalent in aquatic settings (Horton et al. 2017, Koelmans et al. 2019). These results, however, are not in concordance with results reported for the Potomac River, to which Four Mile Run is a tributary (Rhoades et al. 2019). Fibers have been shown to be a major component of treated wastewater effluent (Le Tarte et al. 2019, Leslie et al. 2017), and they account for the overwhelming majority of airborne microplastics (Dris et al. 2017, Dris et al. 2016). Since fibers were abundant in Four Mile Run well above the influence of the tide at the confluence of Long Branch Creek, sources other than treated wastewater are implicated.

The microplastic particle counts, expressed as 0.01-0.24 particles L^{-1} (mean 0.08, median 0.07) show that Four Mile Run has relatively high levels of microplastic pollution compared to similarly situated urban streams. The counts are higher than those reported for waterways in the Chicago metropolitan area ($\leq$0.006 particles L^{-1}, Hoellein et al. 2017; and $\leq$0.018 particles L^{-1}, McCormick et al. 2016, McCormick et al. 2014) and urban tributaries to the Great Lakes ($\leq$0.013 particles L^{-1}, Baldwin et al. 2016), though very similar in range to findings for the Ottawa River (0.05-0.24 particles L^{-1}, Vermaire et al. 2017). They are substantially lower than results obtained for the heavily-urban San Gabriel River (0.411 particles L^{-1} for the comparable microplastic particle size class, Moore et al. 2014), and

somewhat lower than those obtained in a small non-peer-reviewed study conducted at Four Mile Run (0.2-0.9 particles L^{-1}, Libelo and Gallagher 2018).

The counts from the present study are higher than those reported for the nearby waters of Great Hunting Creek and the Potomac and Anacostia rivers ($\leq$0.005 particles L^{-1}, Rhoades et al. 2019), and substantially higher than those for tributaries of the Chesapeake Bay ($\leq$0.001 particles L^{-1}, Yonkos et al. 2014). Some of the difference may be because the sampling in the latter two studies was conducted from boats, from the surface of higher-order waterways. Another likely factor is that the watersheds in those studies had lower population densities and less impervious land surface cover than at Four Mile Run, which is more toward the urban end of an urban-rural land use gradient.

Particle counts for samples taken well upstream of Arlington's wastewater facility and above any tidal influence contained microplastics in abundance, demonstrating that wastewater is not the only important source. Although the present study was unable to show a difference between samples based on recent rainfall, litter and other plastic items washed from streets to storm drains are a potential source, and there are numerous storm drain outfalls throughout the Run. Airborne microplastics may also be important (Prata 2018, Dehghani et al. 2017, Dris et al. 2017, Dris et al. 2016).

Our two wastewater effluent samples had particle counts far exceeding those reported in a comparable study for six wastewater treatment plants discharging to Lake Champlain (means ranging between 0.0006 and 0.0026 particles L^{-1}, with a maximum count of 0.018 particles L^{-1}, Le Tarte et al. 2019). It is possible that our samples were not representative of the typical discharge concentration, and/or the results may reflect differences in the treatment facilities themselves; among other differences, the daily discharge from Arlington's Water Pollution Control Plant is five times that of the largest of the Lake Champlain treatment plants. In contrast, a study of wastewater treatment facilities in the Netherlands reported particle counts for the equivalent particle size class (0.3-5.0 mm) that were much higher (ranging from 0-101 particles L^{-1}, mean 26 particles L^{-1}, Leslie et al. 2017). That study differed significantly in methodology, with neither wet peroxide digestion nor density separation prior to filtration and visual identification, and again, differences in treatment systems may be a factor in the higher counts.

A rough approximation of the amount of microplastic carried by Four Mile Run annually is estimated from the median microplastic concentration in the environmental water samples (12 µg L^{-1}, with the wastewater treatment effluent samples excluded) and multiplying by the median annual flow of the run (16,524,864 m^3 yr^{-1} at the USGS gauge, above the wastewater treatment plant and tide), to reach an estimate of 200 kg yr^{-1}, excluding the amount conveyed by the wastewater treatment plant. This figure is likely an overestimation, as the samples in the tidal reach would be a mixture of Four Mile Run water and wastewater treatment effluent, influenced by tidal mixing.

A similar estimate of the annual microplastic contribution of the wastewater treatment plant is made using the low microplastic figure (100 µg L^{-1}) and the daily wastewater treatment flow to reach a total of 3,200 kg yr^{-1}, an order of magnitude above

the preceding estimate. Further study could verify the extent to which treated wastewater effluent accounts for the total amount of microplastic flowing from Four Mile Run to the Potomac River, but our data suggest it is substantial, especially because the treatment plant's annual outflow is nearly double the median annual flow of the Run itself.

Implications of study method for volunteer-based and citizen science

Modifying a metal bucket by drilling holes or cutting notches so that it drains to a known/measured volume is a low-cost approach well-suited to field sampling by volunteers. It is important to make cuts/holes on only one side, so that the sample can easily be poured from the opposite side without spilling. A watering can could be similarly modified, though it would be more difficult to inspect/clean. The sample size of 100 L is easily collected by this method; a larger sample size, however, would be less practical, due to potential for fatigue while hoisting/pouring repeatedly and for mis-counting the number of draws.

The 100 L samples used in the present study were sufficient for detecting microplastics in quantities that can be easily counted and classified in a basic chemistry lab, such as a school facility. In a less urban setting, the sample amount would surely need to be larger, consistent with the recommendations of Koelmans et al. 2019. Although it worked well for particle counts, the sample size was too small for a good comparison of microplastics by weight. Measured mass is a proper quantitative measure, whereas particle counts are only semi-quantitative, since otherwise identical samples could differ due to breakage of fragments during sampling/processing. Nonetheless, particle counts are a practical and commonly-used methodology that is useful for examining the types and proportions of microplastic materials.

Conducting wet peroxide oxidation without the iron catalyst was chosen to reduce cost and enhance the safety of the lab procedure for volunteers, intended to avoid the higher temperatures and risk of overheating associated with the catalyzed reaction (Masura et al. 2015). For most of the samples, this was indeed the case. However, some of the samples themselves contained iron in sufficient quantity to catalyze the reaction, with the resulting elevated temperature and violent bubbling. A strong such reaction was observed for sample HS 3, which had been collected directly from a large-diameter steel culvert pipe. Because there are many situations which might lead to iron being present in urban streams, we recommend that the wet peroxide oxidation be performed with the iron catalyst, so that the stronger reaction doesn't come as a surprise.

Koelmans et al. (2019) provide guidance on conducting high-reliability microplastic studies. While some of their recommendations are perhaps beyond what a non-profit or citizen-science study would find practical, we believe that incorporating negative and positive controls is a low-cost measure that would help quantify errors attributable to sample contamination and material loss during processing. Although we took pains to minimize the use of synthetic materials, notably clothing, in the field and in the lab, and to keep samples covered as much as possible, it was apparent that microplastic fibers float/drift easily on the slightest of air currents. Loss of microplastic particles through collection/sampling is also possible.

Klein et al. (2018) discuss two potential points of microplastic material loss during wet peroxide oxidation process and sodium chloride density separation. First, hydrogen peroxide is capable of chemical degradation of some plastics (though more characteristically when applied in combination with strong acids or bases), thus it might degrade and reduce the size of particles that otherwise would be in the microplastic size class. Second, during density separation the saturated sodium chloride solution is less dense than some plastics, such as polyvinyl chloride (PVC), so these microplastic particles might settle and be discarded with non-plastic materials. High density particles that might be lost during density separation wouldn't ordinarily be expected to be found in freshwater samples collected at the surface, as with the present study, as the density difference is even greater. Alternatives to simple wet peroxide oxidation and saturated sodium chloride for density separation tend to use materials that are more costly, more toxic, or both, perhaps less feasible for organizations with limited resources.

Visual classification of microplastic materials is commonly used and it demands little in terms of equipment, but it depends on the capabilities of the observer and it may not have the accuracy of other classification methods (Koelmans et al. 2019, Klein et al. 2018). Ideally, visual classification of microplastics could be augmented by spectroscopy or spectrometry, which would also identify the composition of microplastic materials.

CONCLUSIONS

This study provides some insight into the extent of microplastic pollution in a densely populated smaller-order urban stream. It suggests that wastewater treatment effluent is a significant source of microplastic pollution at Four Mile Run, but that it is by no means the only source. Further study of similar smaller-order streams would help determine whether Four Mile Run's level of microplastic pollution is typical for urban impact, and/or whether there are settings from which best practices in preventing microplastic pollution can be learned. Such studies could also shed light on how differences in the categories of microplastics (e.g., fibers) reflect conditions in the watersheds.

Non-profits, friends groups, and citizen scientists can play a role in determining the extent of microplastic contamination of smaller waterways, and they may be able to use this data to sharpen their advocacy and outreach. Though it has limitations as discussed above, the method used in this study is affordable and practical, and it can be enhanced where additional analytical techniques, such as Fourier transform infrared spectroscopy, Raman spectroscopy, and/or mass spectrometry are available to further characterize microplastic samples. Studies using the method here described can help define the problem for waterways too small to sample using conventional towed/stationary nets.

ACKNOWLEDGMENTS

The authors are grateful for the support of the science department at Georgetown Day School for providing lab facilities, equipment, and reagents both summers of the study, and especially for the assistance of Patricia McCole with lab setup. The Four Mile Run Conservatory Foundation would like to thank and acknowledge Leigh Tait with Georgetown Day School and Marianne Hawn with Alexandria City Public Schools for their

coordination of interns in support of this research, and the authors thank Laura Bachle, Alisha Foster, and two anonymous reviewers for their helpful comments on the manuscript.

STATEMENT OF RESPONSIBILITIES

Kurt Moser, corresponding author, conducted and supervised field/lab procedures as principal investigator. Tessa Naughton-Rockwell collected water samples and field data in summer 2019. Ethan Litmans and Louisa Wang collected field samples/data and performed lab analysis in summer 2019. Amanda Manoogian collected field samples/data and performed lab analysis in summer 2018.

LITERATURE CITED

Arlington County, Virginia. 2019. Water Pollution Control Plant, accessed July 25, 2019 at URL https://water.arlingtonva.us/locations/water-pollution-control-plant

Baldwin, A.K., Corsi, S.R., and Mason, S.A. 2016. Plastic debris in 29 Great Lakes tributaries: relations to watershed attributes and hydrology. Environmental Science & Technology 50: 10377-10385

Burns, E.E., and Boxall, A.B. 2018. Microplastics in the aquatic environment: evidence for or against adverse impacts and major knowledge gaps. Environmental Toxicology and Chemistry 37: 2776-2796

Castaneda, R., Avlijas, S., Simard, A., and Ricciardi, A. 2014. Microplastic pollution in St. Lawrence River sediments. Canadian Journal of Fisheries and Aquatic Sciences 71: 1–5

Chae, Y., and An, Y.-J. 2017. Effects of micro- and nanoplastics on aquatic ecosystems: current research trends and perspectives. Marine Pollution Bulletin 124: 624-632

Davey Resource Group. 2017. Urban Tree Canopy Assessment, Arlington County, Virginia

Dehghani, S., Moore, F., and Akhbarizadeh, R. 2017. Microplastic pollution in deposited urban dust, Tehran metropolis, Iran. Environmental Science and Pollution Research 24: 20360–20371

Dris, R., Gasperi, J., Rocher, V., Saad, M., Renault, N., and Tassin, B. 2015. Microplastic contamination in an urban area: a case study in Greater Paris. Environmental Chemistry 12: 592-599

Dris, R., Gasperi, J., Saad, M., Mirande, C., and Tassin, B. 2016. Synthetic fibers in atmospheric fallout: a source of microplastics in the environment? Marine Pollution Bulletin 104: 290-293

Dris, R., Gasperi, J., Mirande, C., Mandin, C., Guerrouache, M., Langlois, V., and Tassin, B. 2017. A first overview of textile fibers, including microplastics, in indoor and outdoor environments. Environmental Pollution 221: 453-458

EcoAction Arlington. 2019. Trash Tally 2019 [Unpublished raw data].

Eriksen, M., Mason, S., Wilson, S., Box, C., Zellers, A., Edwards, W., Farley, H., Amato, S. 2013. Microplastic pollution in the surface waters of the Laurentian Great Lakes. Marine Pollution Bulletin 77(1-2): 177-182

Fry, J., Xian, G., Jin, S., Dewitz, J., Homer, C., Yang, L., Barnes, C., Herold, N., and Wickham, J. 2011. Completion of the 2006 National Land Cover Database for the

Conterminous United States. Photogrammetric Engineering & Remote Sensing 77(9): 858-864

Herzke, D., Anker-Nilssen, T., Nøst, T.H., Götsch, A., Christensen-Dalsgaard, S., Langset, M., Fangel, K., and Koelmans, A.A. 2016. Negligible impact of ingested microplastics on tissue concentrations of persistent organic pollutants in Northern Fulmars off coastal Norway. Environmental Science & Technology 50(4): 1924-1933

Hall, N.M., Berry, K.L.E., Rintoul, L., and Hoogenboom, M.O. 2015. Microplastic ingestion by scleractinian corals. Marine Biology 162: 725–732

Hoellein, T.J., McCormick, A.R., Hittie, J., London, M.G., Scott, J.W., and Kelly, J.J. 2017. Longitudinal patterns of microplastic concentration and bacterial assemblages in surface and benthic habitats of an urban river. Freshwater Science 36(3): 491-507

Horton, A.A., Walton, A., Spurgeon, D.J., Lahive, E., Svendsen, C. 2017. Microplastics in freshwater and terrestrial environments: evaluating the current understanding to identify the knowledge gaps and future research priorities. Science of the Total Environment 586: 127–141

Klein, S., Dimzon, I.K., Eubeler, J.P., and Knepper, T. 2018. Analysis, occurrence, and degradation of microplastics in the aqueous environment. In Wagner, M., and Lambert, S. (eds.), Freshwater Microplastics: Emerging Environmental Contaminants. Springer International Publishing AG, Switzerland, pp. 51-68

Koelmans, A.A., Besseling, E., Shim, W.J. 2015. Nanoplastics in the aquatic environment. Critical review. In Bergmann, M., Gutow, L., Klages, M. (eds.), Marine Anthropogenic Litter. Springer International Publishing AG, Switzerland, pp. 325-340

Koelmans, A.A., Mohamed Nor, N.H., Hermsen, E., Kooi, M., Mintenig, S.M., and De France, J. 2019. Microplastics in freshwaters and drinking water: critical review and assessment of data quality. Water Research 155: 410-422

Leslie, H.A., Brandsma, S.H., van Velzen, M.J.M., Vethaak, A.D. 2017. Microplastics en route: Field measurements in the Dutch river delta and Amsterdam canals, wastewater treatment plants, North Sea sediments and biota. Environment International 101:133–142

Le Tarte, L., McCauley, N., Moriarty, M., Lee, E., Brown, S., Buksa, B., Niekrewicz, T., Barnes, J., and Chaskey, E. 2019. Microplastic pollution: a survey of wastewater effluent in the Lake Champlain basin. Student research poster/presentation, Center for Earth and Environmental Science and Department of Biology, SUNY Plattsburgh.

Libelo, H., and Gallagher, J. 2019. Microplastics in a suburban stream. Student poster/presentation at the 39th annual meeting of the Society of Environmental Toxicology and Chemistry of North America, Sacramento, California.

Masura, J., Baker, J.E., Foster, G.D., Arthur C., and Herring, C. 2015. Laboratory methods for the analysis of microplastics in the marine environment : recommendations for quantifying synthetic particles in waters and sediments. NOAA Marine Debris Program Technical Memorandum NOS-OR&R-48

Mato, Y., Isobe, T., Takada, H., Kanehiro, H., Ohtake, C., and Tsuguchika, K. 2001. Plastic resin pellets as a transport medium for toxic chemicals in the marine environment. Environmental Science & Technology 35:318–324

McCormick, A., Hoellein, T.J., Mason, S.A., Schluep, J., and Kelly, J.J. 2014. Microplastic is an abundant and distinct microbial habitat in an urban river. Environmental Science & Technology 48: 11863–11871

McCormick, A.R., Hoellein, T.J., London, M.G., Hittie, J., Scott, J.W., and Kelly, J.J. 2016. Microplastic in surface waters of urban rivers: concentration, sources, and associated bacterial assemblages. Ecosphere 7(11): e01556

Moore, C.J., Lattin, G.L., and Zellers, A.F. 2011. Quantity and type of plastic debris flowing from two urban rivers to coastal waters and beaches of Southern California. Journal of Integrated Coastal Zone Management 11(1): 65-73

Nguyen, H., Rhoades, B., Wigode, E., Hutchinson, T., Foster, G., and Sklarew, D. 2019. Microplastics' composition and role as vectors for persistent organic pollutants. Presentation/poster, Potomac Science Center, 2 August 2019

Northern Virginia Regional Commission. 2004. Implementation plan for the fecal coliform TMDL (total maximum daily load) for Four Mile Run, Virginia

Prata, J.C. 2018. Airborne microplastics: Consequences to human health? Environmental Pollution 234: 115-126

Rhoades, B., Nguyen, H., Wigode, E., Sklarew, D., and Foster, G. 2019. Microplastics in the tidal freshwater Potomac River. Presentation/poster, Potomac Science Center, 2 August 2019

Rochman C.M., Tahir, A., Williams, S.L., Baxa, D.V., Lam, R., Miller, J.T., Teh, F-C, Werorilangi, S., and Teh, S.J. 2015. Anthropogenic debris in seafood: Plastic debris and fibers from textiles in fish and bivalves sold for human consumption. Scientific Reports 5:14340

Ryan, P.G. 2015. A brief history of marine litter. In Bergmann, M., Gutow, L., Klages, M. (eds.), Marine Anthropogenic Litter. Springer International Publishing AG, Switzerland, pp. 1-25

Smith, M., Love, D.C., Rochman, C.M., and Neff, R.A. 2018. Microplastics in seafood and the implications for human health. Current Environmental Health Reports 5: 375–386

Sussarellu, R., Suquet, M., Thomas, Y., Lambert, C., Fabioux, C., Pernet, M.E.J., Le Goïc, N., Quillien, V., Mingant, C., Epelboin, Y., Corporeau, C., Guyomarch, J., Robbens, J., Paul-Pont, I., Soudant, P., and Huvet, A. 2016. Oyster reproduction is affected by exposure to polystyrene microplastics. Proceedings of the National Academy of Sciences of the United States of America 113: 2430–2435

Tanaka, K., Takada, H. 2016. Microplastic fragments and microbeads in digestive tracts of planktivorous fish from urban coastal waters. Scientific Reports 6:34351

Tanaka, K., Takada, H., Yamashita, R., Mizukawa, K., Fukuwaka, M., and Watanuki, Y. 2013. Accumulation of plastic-derived chemicals in tissues of seabirds ingesting marine plastics. Marine Pollution Bulletin 69(1–2): 219-222

U.S. Geological Survey. 2019. National Water Information System data available on the World Wide Web (USGS Water Data for the Nation), accessed October 3, 2019, at URL https://waterdata.usgs.gov/usa/nwis/uv?01652500

Vermaire, J.C., Pomeroy, C., Herczegh, S.M., Haggart, O., Murphy, M. 2017. Microplastic abundance and distribution in the open water and sediment of the Ottawa River, Canada, and its tributaries. Facets 2(1): 301-314

Virginia Department of Environmental Quality. 2018. Final 2016 305(b)/303(d) Water Quality Assessment Integrated Report

Yonkos, L.T., Friedel, E.A., Perez-Reyes, A.C., Ghosal, S., and Arthur, C.D. 2014. Microplastics in four estuarine rivers in the Chesapeake Bay, USA. Environmental Science and Technology 48: 14195-14202

TABLE 1: Results of Four Mile Run microplastic sampling, with precipitation data from the Four Mile Run USGS gage station, microplastic amounts by mass and by particle counts. Sites FM(1-6) are at different locations in the vicinity of the Mount Vernon Avenue bridge; sites HS(1-3) are tidal sites at the Hume Spring tributary; site HS4 is at the Hume Spring stormwater outfall; sites TP(1-2) are at the Arlington Water Pollution Control Plant outfall; sites above the tidal extent are UP1 on Lower Long Branch Creek and site UP2 on the main stem of Four Mile Run, above the confluence of Lower Long Branch Creek.

Site	Date	Rainfall previous 24 hours	Concentration (µg/L)	Total # particles	Fragments	Fibers	Film	Sponge/Foam
Four Mile Run locations near head of tide								
FM1	2018-06-11	1.5cm	55	6	2	1	1	2
FM2	2019-05-20	none	12	8		8		
FM3	2019-05-20	none	21	1		1		
FM4	2019-05-28	0.6 cm	12	13	5	6		2
FM5	2019-06-04	none	12	13		12	1	
FM6	2019-06-08	2.5cm	2	7	1	5		1
Hume Spring tributary locations								
HS1	2018-06-11	1.5cm	265	9	2	4		3
HS2	2019-05-30	0.6 cm	24	24	6	12	2	4
HS3	2019-06-05	none	2	7	4			3
HS4	2019-06-06	none	13	2	2			
Arlington Water Pollution Control Plant								
TP1	2018-06-13	N/A	446	3	2			1
TP2	2019-06-18	N/A	100	7		7		
Four Mile Run and Lower Long Branch Creek above their confluence								
UP1	2019-06-18	2.5 cm	11	5		5		
UP2	2019-06-18	2.5 cm	3	6	1	5		

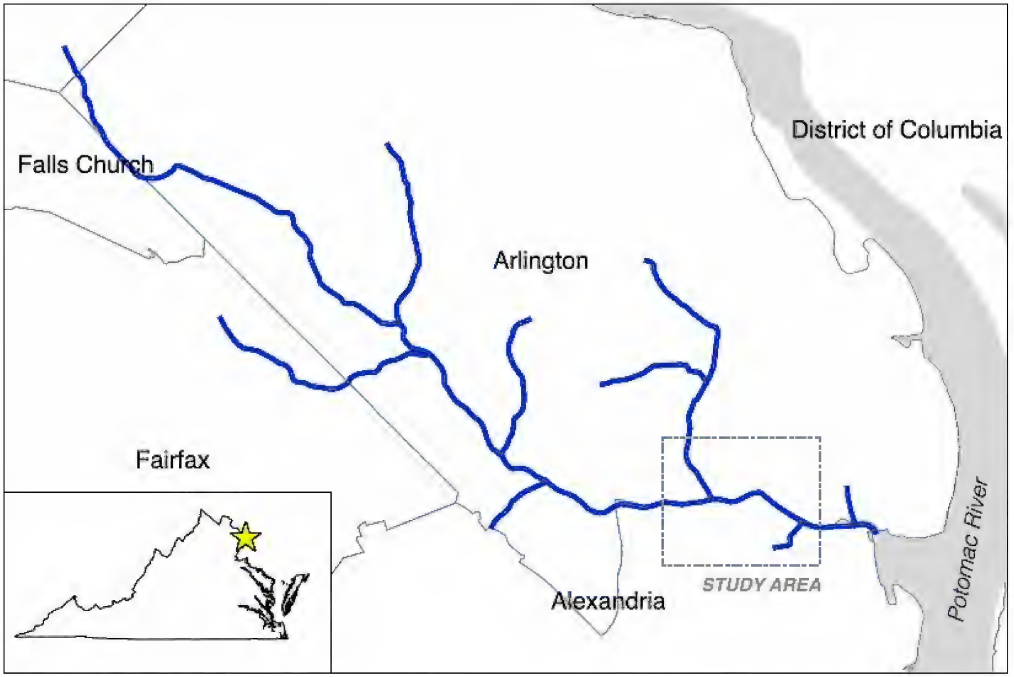

Figure 1: Overview map of Four Mile Run and study area in Alexandria/Arlington, Northern Virginia

Figure 2: Aerial imagery of Lower Four Mile Run showing microplastic sampling locations

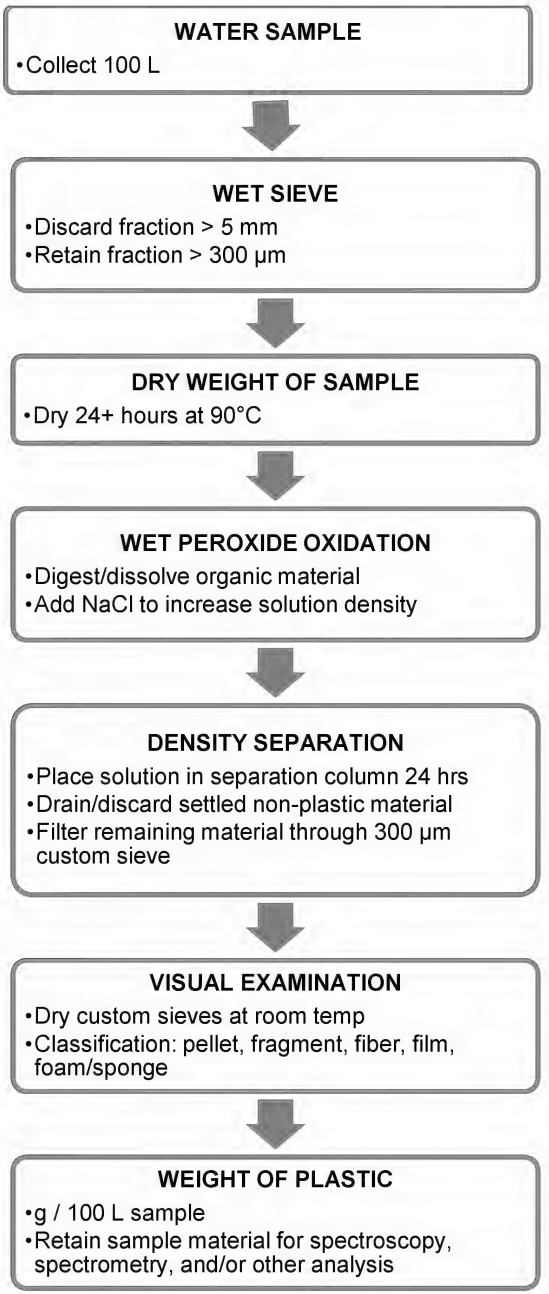

Figure 3: Flow chart of sample collection/analysis procedure

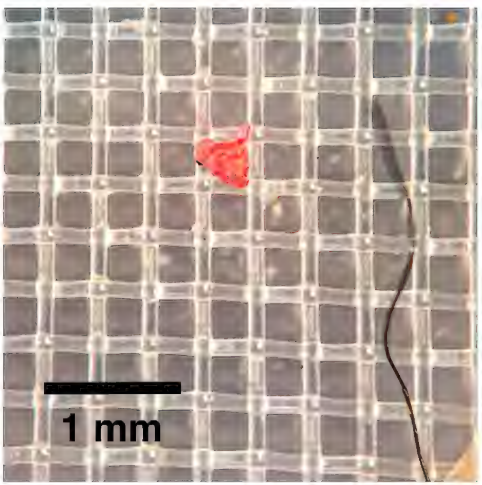

(a)

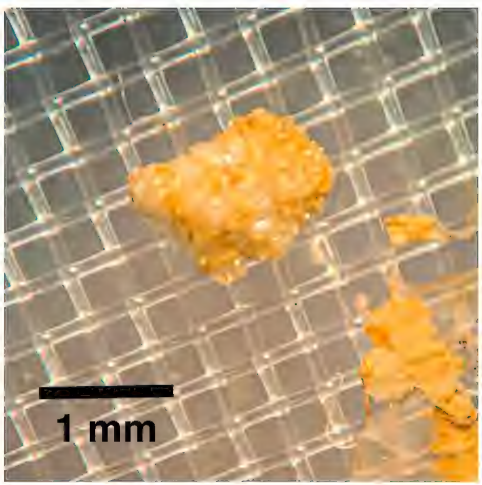

(b)

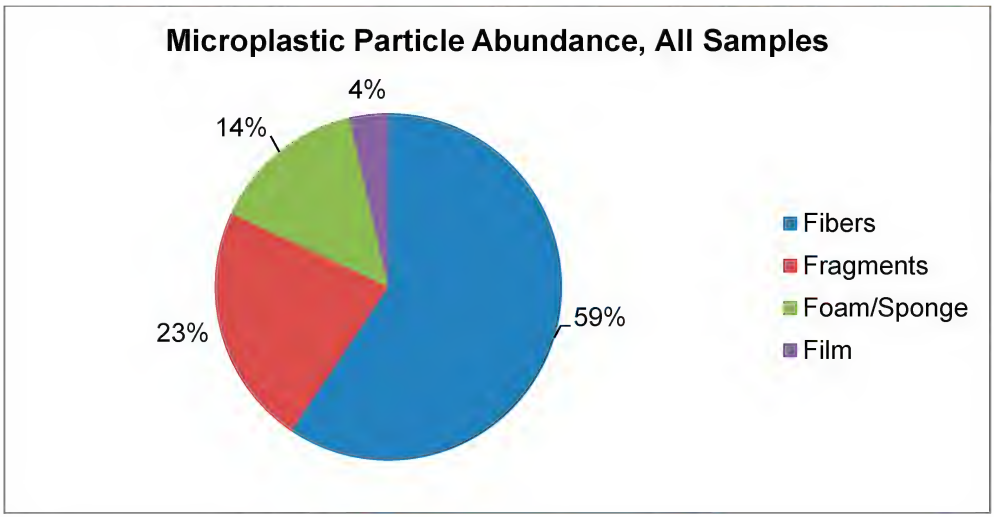

(c)

Figure 4: Microscope photos showing microplastic fragment and fiber (a) and foam particle (b); relative abundances of particles identified for Four Mile Run water samples (c)

Virginia Journal of Science
Volume 71, Issue 1 & 2
Spring & Summer 2020
doi: 10.25778/6hjn-a318

Note: This manuscript has been accepted for publication and is online ahead of print. It will undergo copyediting, typesetting, and review of the resulting proof before it is published in its final form.

Variables Associated with Thermal Emittance of Wall Mural Art in Richmond, Virginia

Sarah Kwon[1] and Eugene G. Maurakis[1,2]

[1]University of Richmond, 410 Westhampton Way, Richmond, VA 23173*
[2]Science Museum of Virginia, 2500 West Broad Street, Richmond, VA 23220

ABSTRACT

The objectives of this research are to determine the factors associated with the minimum, maximum, and average thermal emittance temperatures of wall murals in Richmond, Virginia, and make recommendations for color and location of wall murals. Data for 17 parameters were collected for 64 art murals in downtown Richmond, VA from 28 June 2018 – 19 July 2018. Date, time, solar exposure duration, solar elevation, latitude, longitude, air temperature (C), lux, color, solar cardinal minutes, cardinal direction, minimum, maximum, and average surface thermal emittance temperatures of mural face were recorded for each mural. We reject the hypothesis that minimum, maximum, and average thermal emittance temperatures of wall murals do not vary significantly with temporal, spatial, physical changes, and solar factors. Maximum, minimum, and average emittance temperatures of wall mural art varied significantly with the number of minutes that solar energy directly illuminating mural art for each cardinal direction, lux, solar elevation, total diurnal exposure, maximum mural color, and percent dark colors on murals. Minimum mural wall art temperatures (30.0-37.0 C) occurred on surfaces facing East, North, Northwest, and Northeast which also had the lowest lux values (8,867-14,231); highest temperatures (44.8-49.9 C) were recorded on walls facing South, Southeast, and West, which had the highest lux values (42,517-46,000). Based on results of this study and those investigating mitigation of the urban heat island effect with building materials and coatings on walls and roofs, we recommend a study that uses a systematic approach to locating wall mural art based on specific colors, paint composition, and wall materials to guide local building authorities owners, and artists to maximize albedo. Additionally, we recommend, where possible, mural art should be painted on vertical surfaces facing North, Northeast, and Northwest where

* Graduated from the University of Richmond in 2019. Sarah is currently working at the Keck Center for the National Academies of Sciences, Engineering, and Medicine: 500 5th St NW, Washington, DC 20001

lux values and thermal gain are the lowest of all possible cardinal directions. Such locations could accommodate the use of dark colors without significantly increasing the heat load in urban communities. And finally, where mural art is being considered for building walls facing South, Southeast, Southwest and West, we recommend that artists use a palette of primarily light colors with high reflective properties to maximize albedo, and minimize use of dark colors.

INTRODUCTION

Hundreds of metropolitan areas around the world experience warmer temperatures compared to surrounding rural lands (Fox et al., 2018). Rapid urbanization has caused these warmer microclimates to develop through a phenomenon known as the Urban Heat Island effect (UHI), which is particularly acute during warmer months (Nuruzzaman, 2015). Urban Heat Islands are a result of human modification of land surfaces (e.g. asphalt roads, parking lots, non-reflective roofs) related to urban sprawl (Fox et al., 2918). Vegetation and open spaces are replaced by buildings and pavements which absorb and retain solar energy more than green environments, increasing the ambient air temperature of an urban area. UHI effects have been demonstrated to exacerbate livability and human health during the summer months resulting in increased heat-related illnesses, such as dehydration, heat exhaustion, heat cramps, heat syncope, and heat strokes (Lugo-Amador et al., 2004), as well as increased cooling costs (Pisello, 2017).

External surface temperature of buildings is a key factor in UHI because solar energy absorbed by buildings is radiated back into the atmosphere, and intensifies the heat within cities (Fox et al., 2018). Therefore, finding effective and innovative ways to increase solar reflectance of surfaces or albedo has become a major concern in metropolitan areas. Many studies have been conducted to mitigate the effects of UHI by increasing albedo. 'Cool' materials such as cool roofs, paints, and pavements have recently gained interest due to their high reflectivity and cost-effectiveness to mitigate UHI. For example, in thermal performance tests of 10 prototypes, containing near-infrared reflective color pigments, Synnefa et al. (2011) determined that cool colored coatings had solar reflectance values higher than conventional colored coatings, which resulted in maintaining a lower surface temperature. Zinzi (2016) found that near-infrared reflective paints have been proven to be effective on building facade application by reducing cooling energy uses from 10-20%, reducing peak operative temperatures by 0.5 to 1.6 °C for buildings in free floating conditions, and by reducing external surface temperatures up to 6°C. Akbari et al. (2009) and Akbari et al. (2012) discovered that by installing cool roofs and pavements (highly reflective surfaces) globally, can lead to an offset of 44 Gt CO_2. Akbari et al. (2012) continued their studies in CO_2 offsets and determined that increasing the albedo of metropolitan areas resulted in global cooling occurred from 0.01 to 0.07 K, corresponding to 25 to 150 billion tonne reduction in CO_2 emission. Additionally, Sproul et al. (2014) found that by replacing black tops with white tops on residential buildings, there was a 50-year net saving in energy costs of \$25/m^2 relative to the black tops due to increased solar reflectance.

Although there are multiple studies on how cool materials and pavements are able to mitigate the effects of UHI, there is little to no research in how street art and building murals affect external surface heat absorption. With many urban areas concerned about the aesthetics of the city, street murals have become an essential part of city design and life (Weber et al., 2008). Yet street murals have not been investigated in terms of heat absorption mainly because the research focus has been on solar radiation impacts on horizontal surfaces rather than vertical surfaces. Other than a newspaper report by Thompson and Byrne (2017) suggesting that street art decreases indoor temperatures of buildings across the street, there is no published research on the factors associated with mural wall art temperatures on vertical surfaces of buildings in urban areas. The objectives of this research are to determine the factors associated with the minimum, maximum, and average temperatures of wall murals in Richmond, Virginia, and make recommendations for color and location of wall murals. The hypothesis is that minimum, maximum, and average thermal emittance temperatures of wall murals do not vary significantly with changes in date, time, location, solar exposure and elevation, air temperature, cardinal direction, lux, and light and dark surfaces of murals.

MATERIALS AND METHODS

Data for 17 parameters were collected for 64 art murals in downtown Richmond, VA on cloudless to near cloudless days (okta[1] range 0-1) from 28 June 2018 – 19 July 2018. Date, time, solar exposure duration (total daylight minutes/day), solar elevation (degrees), latitude, longitude, air temperature (C), solar cardinal minutes (number of minutes striking a vertical wall facing each cardinal direction, Fig. 1), and cardinal direction of mural face (degrees) were recorded for each mural. ArcGIS was used to verify cardinal directions and solar cardinal minutes of each mural initially generated from Google Street View. Solar exposure and elevation were derived from the NOAA Solar Position Calculator of the Earth System Research Laboratory, Global Monitoring System at the Department of Commerce. Air temperature was obtained for Richmond, VA from historical temperature data archives from the National Weather Service Forecast Office in Wakefield, VA. Distributions of minimum, maximum, and average surface thermal emittance temperatures (C) of each wall mural were recorded using a thermal imaging camera (Flir One Gen 3 Pro camera for android phones) with an error range of approximately +/- 3° C. Wall thermal emittances were recorded *in situ* from 12 pm to 4 pm. Lux (luminous flux/area) striking the surface of each mural was recorded using an AEMC Model1110 Light Meter Data Logger. Light and dark colors on each mural were assigned a value from 1-10 (1=white, 10=black) and used to calculate percent dark color and color preference (scale 0-1), where:

$$\text{Color preference} = \frac{(\text{dark value} - \text{light value})}{(\text{dark value} + \text{light value})}$$

A fixed grid in the Flir® Tools and Report Studio software was used to calculate the total number of dark and light color areas on murals and generate a dark color percentage for each mural.

[1] Unit of measurement describing cloud coverage. Okta ranges from 0 (clear sky) to 8 (complete cloud coverage)

Correlation analyses (SAS 2018) calculated Pearson correlation coefficients to determine significant relationships among all parameters (p=0.05). A General Linear Model followed by Duncan's Multiple Range Test (SAS 2018) was used to determine significant differences for each parameter (p=0.05) by cardinal direction. Rotated factor patterns derived from factor analyses (SAS 2018) were used to determine the groups of parameters accounting for signification variation for each of the minimum, maximum, and average thermal emittance temperatures of wall murals.

RESULTS

South-facing murals receive sunlight for the entirety of the day, absorbing the most solar radiation, whereas North-facing murals are not in the sun's path except early in the morning and late in the evening in the summer and receive the least amount of solar radiation.

Minimum, maximum, and average temperatures of murals were significantly positively correlated with each other at $p<0.001$, and with solar cardinal direction ($p<0.001$), air temperature ($p=0.009$, 0.05, and 0.02, respectively), and lux ($p=0.06$, <0.001, and 0.001, respectively; Table 1). Lux was significantly correlated with solar exposure ($p=0.001$) and solar cardinal direction ($p<0.001$; Table 1).

Average maximum temperatures (44.7-50.0 C) of murals facing South, Southeast, Southwest, and West were significantly higher than those (30.6-42.6 C) painted on walls facing North, Northeast, and Northwest (Table 2; Fig. 2, 3 and 4). Average minimum temperatures (33.0-37.3 C) of murals facing West, Southwest, Southeast, East, and South were significantly higher than those (26.3-30.8 C) facing North (Table 3; Fig. 2, 3 and 4). Average temperature of murals facing North was significantly lower than those facing Southwest, East, West, Southeast, and South (Table 4; Fig. 2, 3 and 4). Average lux values (45,600-46,000) measured at mural surfaces facing West and South were significantly higher than those (8,867-21,839) facing Southeast,, Northeast, Northwest, North, and East ((Table 5; Fig. 5). Average solar exposure (882 min) at mural surfaces facing East were significantly greater than those facing West (875.6 min) (Table 6).

There were no significant differences among average values of air temperature (avg. range=32.0-33.3 C), solar elevation (avg. range=64.7-70.7), percent dark areas on murals (avg. range=36.7-58.3), minimum colors of murals (avg. range=1.0-1.7) maximum colors of murals (avg. range=9.7-10.0), and preference of dark to light areas on wall murals (Table 7) among all cardinal directions and wall murals.

Factor analysis indicated that the first three factors accounted for 80.9 percent of the variation in the maximum temperature of wall mural art (Table 8). Factor 1 (maximum temperature, solar cardinal minutes striking mural art, and lux) contributed 32.8 % of the variation in maximum wall mural art temperature; Factor 2 (maximum color of mural, solar elevation) contributing 26.5 % of the variation in the maximum wall mural art temperature; and Factor 3 (total diurnal exposure, and percent dark colors on murals) contributed 21.5% of the variation in maximum wall art temperature (Table 8).

For minimum temperatures of wall mural art, factor analysis indicated that the first three factors accounted for 80.1 percent of the variation in minimum temperatures (Table 9). Factor 1 (maximum temperature, solar cardinal minutes striking mural art, and lux) contributed 28.7 % of the variation in maximum wall mural art temperature; Factor 2 (maximum color of mural, solar elevation) contributing 27.2 % of the variation in the maximum wall mural art temperature; and Factor 3 (total diurnal exposure, and percent dark colors on murals) contributed 24.2% of the variation in maximum wall art temperature (Table 9).

Factor analysis results for average temperatures of wall mural art indicated the same three Factors as in those for maximum and minimum temperatures of wall mural art accounted for 80.7 percent of the variation in average temperatures of wall mural art (Table 10). Factor 1 accounted for 31.6% of the variation in average wall temperature; Factor 2 contributed 26.6 %, and Factor 3 contributed 22.5 % (Table 10).

DISCUSSION

We reject the hypothesis that minimum, maximum, and average thermal emittance temperatures of wall murals do not vary significantly with changes temporal, spatial, physical, and solar factors. Maximum, minimum, and average emittance temperatures of wall mural art varied significantly with the number of minutes that solar energy directly illuminating mural art for each cardinal direction, lux, solar elevation, total diurnal exposure, maximum mural color, and percent dark colors on murals (Table 1). Minimum mural wall art temperatures (30.0-37.0 C) occurred on surfaces facing East, North, Northwest, and Northeast which also had the lowest lux values (8,867-14,231) (Figs. 4 and 5); highest temperatures (44.8-49.9 C) were recorded on walls facing South, Southeast, and West, which had the highest lux values (42,517-46,000) **(**Figs. 4 and 5**).**

Although average solar elevation angle (64.7-70.7), dark mural color rank (9.7-10), and percent dark mural color (36.7-58.3) did not vary significantly with cardinal direction, they did contribute to the variation in data in factor analyses (Tables 8-10). The amount of solar energy per unit area striking surfaces has been demonstrated to vary with solar elevation (Ruelas, 2017). Solar elevation angle is one of the most important factors for parameterizing surface albedo (Zheng et al., 2017). In a study of white, green, and black flat roofs, Sproul et al. (2014) indicated that white and "green" (vegetated) roofs have begun replacing conventional black (dark-colored) roofs to mitigate the adverse effects of dark impervious urban surfaces.

Likewise, air temperature was a significant factor accounting for the variation in wall mural art temperatures (32.0-33.3 C) albeit it did not vary significantly with cardinal direction (Tables 8-10). Thermal lag time between solar flux and ambient air temperature, longwave radiation energy, and heat storage of vertical walls may account for the higher temperatures of wall mural art facing South, Southeast, and West. Banyal et al. (2013) determined that peaks of solar flux and ambient temperature are shifted by two hours due to thermal time lag. Longwave radiation energy (heat emitted from ground surfaces surrounding the vertical faces of buildings) (Engineering Reference, 2018) and climatic conditions (e.g. summer air temperatures), used in calculations of thermal insulation and

heat storage of exterior building materials (Long and Ye, 2016) are factors that impact air temperature, and may have affected the maximum temperature of wall murals.

Numerous studies have focused on the effects of building facades and materials (including those of historic buildings), cool coatings, high albedo colors, and reflective materials to mitigate urban heat island effects (Becherini et al., 2018; Fox et al, 2018; Mauri et al, 2018; Pisello, 2017; Zinzi, 2016; Rossi et al., 2015; and Hernandez-Perez et al., 2014). This includes the question of heat dispersion when light is reflected off of a high-albedo surface. (Dupuis 2013, Ibrahim 2013, Jacobson 2012). Although Jacobson 2012 found that installation of white roofs increased overall global temperatures, there are little to no literature on vertical surfaces increasing global temperatures, in part due to the complexities and variability of irradiation of vertical and titled surfaces (Maxwell et al., 1986). Algorithms for measuring vertical surface irradiation can also be highly inaccurate (Maxwell et al., 1986). However, there are studies and examples that show vertical surfaces having an impact on the surrounding, local air temperatures (Price, 2015, Zinzi 2016, Fox et al. 2018, Thompson, J. & C. Byrne. 2017).

Based on results of this study and those investigating mitigation of the Urban Heat Island effect with building materials and coatings on walls and roofs, we recommend a study that uses a systematic approach to locating wall mural art based on specific colors, paint composition, and wall materials to guide local building authorities owners, and artists to maximize albedo. Additionally, we recommend, where possible, mural art should be painted on vertical surfaces facing North, Northeast, and Northwest where lux values and thermal gain are the lowest of all possible cardinal directions. Such locations could accommodate the use of dark colors without significantly increasing the heat load in urban communities. And finally, where mural art is being considered for building walls facing South, Southeast, Southwest and West, we recommend that artists use a palette of primarily light colors with high reflective properties to maximize albedo, and minimal use of dark colors. Our recommendations are consistent with the findings of Becherini et al. (2018); Fox et al. (2018); Mauri et al. (2018), Pisello (2017); Zinzi (2016); Rossi et al. (2015); Hernandez-Perez et al. (2014), and Synnefa et al. (2011) who determined that cool colored coatings on vertical surfaces of buildings have solar reflectance values higher than conventional colored coatings, resulting in lower surface temperatures. Zinzi (2016) and Revel et al. (2014) both show that cool materials on vertical surfaces can have a significant impact on lowering energy use due to reduced thermal absorption. Although cool colored paints have gained attention over the years, artists are probably unlikely to use cool colored paints due to their higher cost and limited availability. However, conventional paints may also have unexpected benefits and consequences that affect the amount of heat being absorbed into the city. For example, Tukiran et al. (2015) found that cool-colored asphalt and concrete pavements all had lower surface temperature compared to conventional or uncoated pavements, even though the paints did not have near-infrared reflective pigments.

LITERATURE CITED

Akbari, H., H.D. Matthews, and D. Seto. 2012. The long-term effect of increasing the albedo of urban areas. Environmental Research Letters. 7:1-10.

Akbari, H., S. Menon and A. Rosenfeld. 2009. Global cooling: increasing world-wide urban albedos to offset CO_2. Climatic Change. 94:275-286.

Banyal, R., B. Ravindra, and S. Chatterjee. 2013. Opto-thermal analysis of a lightweighted mirror for solar telescope. Optics Express 21(6):7065-7081.

Becherini, F. E. Lucchi, A. Gandini, M. C. Barrasa, A. Troi, F. Roberti, M. Sachini, M, Concetta Di Tuccio, L. G. Arrieta, L. Pockele, and A. Bernardi. 2018. Characterization and thermal performance evaluation of infrared reflective coatings compatible with historic buildings. Buildings and Environment. 134 (2018):35-46.

Engineering Reference. 2018. Outside surface heat balance. Big EnergyPlus Web-based Documentation. Version 9. BigLadder Software, LLC. 20 p. https://bigladdersoftware.com/epx/docs/8-0/engineering-reference/page-020.html

Fox, J., P. Osmond, and A. Peters. 2018. The effect of building facades on outdoor microclimate – Reflectance recovery from terrestrial multispectral images using a robust empirical line method. Climate. 6(3):1-27. http://dx.doi.org.newman.richmond.edu:2048/10.3390/cli6030056

Hernandez-Perez, I., G. Alvarez, J. Xaman, I. Zavala-Guillen, J. Arce, and E. Sima. 2014. Energy and Buildings. 80(2014):81-105.

Lugo-Amador, N. M., T. Rothenhaus, and P. Moyer. 2004. Heat-related illness. Emergency Medicine Clinics of North America. 22:315–327.

Mauri, L., G. Battista, E. de Lieto Vollaro, and R. de Lieto Vollaro. 2018. Retroreflexive materials for buildings' facades: Experimental characterization and numerical simulations. Solar Energy. 171:150-156.

Maxwell, E.L. & Stoffel, Thomas & Bird, R.E.. (1986). Measuring and modeling solar irradiance on vertical surfaces. 10.2172/5439042.

Nuruzzaman, Md. 2015. Urban Heat Island: Causes, Effects and Mitigation Measures - A Review. International Journal of Environmental Monitoring and Analysis. 3(2): 67-73.

Pisello, A. L. 2017. State of the art on the development of cool coatings for buildings and cities. Solar Energy. 144(2017):660-680.

Price, Alexandra & Jones, Erick & Jefferson, Felicia. (2015). Vertical Greenery Systems as a Strategy in Urban Heat Island Mitigation. Water, Air, and Soil Pollution. 226. 10.1007/s11270-015-2464-9.

Revel, G.M., M. Martarelli, M. Emiliani, L. Celotti, R. Nadalini, A.D. Ferrari, S. Hermanns, and E. Beckers. 2014. Cool products for building envelope – Part II: Experimental and numerical evaluation of thermal performances. Solar Energy. 105:780–791.

Rossi, F., B. Castellani, A. Presciutti, E. Morini, M. Filipponi, A. Nicolini, and M. Santamouris. Retroflective facades foro urban heat island mitigation: Experimental investigation and energy evaluations. Applied Energy. 145(2015):8-20.

Ruelas, A., N. Velázquez, C. Villa-Angulo, A. Acuña, P. Rosales, and J. Suastegui. 2017. A Solar Position Sensor Based on Image Vision. Sensors (Basel). 17(8):1742-1759.

SAS. 2018. SAS User Guide, version 9.4. SAS Institute, Cary, NC. 484 p.

Sproul, J., M.P. Wan, B. H. Mandel, and A. H. Rosenfeld. 2014. Economic comparison of white, green, and black flat roofs in the United States. Energy and Buildings. 71:20–27.

Stempihar, J. J., T. Pourshams-Manzouri, K. E. Kaloush, and M.C. Rodezno. 2012. Porous Asphalt Pavement Temperature Effects for Urban Heat Island Analysis. Transportation Research Record: Journal of the Transportation Research Board. 2293:123–130.

Synnefa, A., T. Karlessi, N. Gaitani, M. Santamouris, D. N. Assimakopoulos, and C. Papakatsikas. 2011. Experimental testing of cool colored thin layer asphalt and estimation of its potential to improve the urban microclimate. Building and Environment. 46:38–44.

Thompson, J. and C. Byrne. 2017. Darwin temperature drop stumps business, suggesting street art is cooler than we think. ABC Radio Darwin. https://www.abc.net.au/news/2017-11-29/darwin-temperature-drop-street-art-blamed/9206058

Tukiran, Md., J. Ariffin, J. Abdul, and A. N. Ghani. 2016. Comparison on colored coating for asphalt and concrete pavement based on thermal performance and cooling effect. Journal Teknologi. 78(5):63-70.

Weber, R., J. Schnier and T. Jacobsen. 2008. Aesthetics of street art: influence of fundamental properties on aesthetic judgments of urban space. Journal of Perceptual and Motor Skills. 106(1):128-46.

Zheng Z., Z. Wei, Z. Wen, W. Dong, Z. Li, X. Wen, X. Zhu, D. Ji, C. Chen, and D. Yan. 2017. Inclusion of solar elevation angle in land surface albedo parameterization over bare soil surface. Journal of Advances in Modeling Earth Systems, 9, 3069–3081. https://doi.org/10.1002/2017MS001109

Zinzi, M. 2016. Characterisation and assessment of near infrared reflective paintings for building facade applications. Energy and Buildings. 114:206–213.

TABLES

TABLE 1. (See Table 1 data as a separate file) Results of Pearson correlation analyses among 17 factors collected for wall art murals in Richmond, Virginia during June - July, 2018.

TABLE 2. Results of Duncan's Multiple Range Test for maximum mural thermal emittance temperature (C) based on a general linear model analysis of variance. Underscored means do not differ significantly at p=0.05.

Cardinal	North	Northwest	Northeast	East	West	Southwest	Southeast	South
N	2	12	8	3	2	12	22	3
Mean	30.56	36.16	37.04	42.61	44.80	45.18	45.53	49.98

TABLE 3. Results of Duncan's Multiple Range Test for minimum mural thermal emittance temperature (C) based on a general linear model analysis of variance. Underscored means do not differ significantly at p=0.05.

Cardinal	North	Northeast	Northwest	West	Southwest	Southeast	East	South
N	2	8	12	2	12	22	3	3
Mean	26.33	30.57	30.83	32.97	33.69	35.29	36.07	99.17

TABLE 4. Results of Duncan's Multiple Range Test for average mural thermal emittance temperature (C) based on a general linear model analysis of variance. Underscored means do not differ significantly at p=0.05.

Cardinal	North	Northwest	Northeast	Southwest	East	West	Southeast	South
N	2	12	8	12	3	2	22	3
Mean	28.53	33.55	34.01	38.91	39.63	40.22	40.45	44.50

TABLE 5. Results of Duncan's Multiple Range Test for lux based on a general linear model analysis of variance. Means underscored by the same line do not differ significantly at p=0.05.

Cardinal	East	North	Northwest	Northeast	Southeast	Southwest	South	West
N	3	2	12	8	22	12	3	2
Mean	8,867	9,400	10,845	14,231	21,839	42,517	45,600	46,000

TABLE 6. Results of Duncan's Multiple Range Test for solar exposure duration (minutes) based on a general linear model analysis of variance. Underscored means do not differ significantly at p=0.05.

Cardinal	West	North	South	Southwest	Southeast	Northwest	Northeast	East
N	2	2	3	12	22	12	8	3
Mean	875.6	875.6	875.9	878.3	879.7	14.66252	880.6	882.0

TABLE 7. Non-significant results derived from Duncan's Multiple Range Test for air temperature (C), solar elevation, % dark, minimum light, and maximum dark colors of murals, and color preference index values based on a general linear model analysis of variance. Means do not differ significantly at p=0.05.

Parameter	n	Average range	F	Pr>F
Air temperature	63	32.0 - 33.3	1.09	0.3832
Solar elevation	63	64.7 - 70.7	1.78	0.1103
% dark mural color	63	36.7 - 58.3	0.77	0.6142
Minimum light color	63	1.0 - 1.68	0.39	0.9030
Maximum dark color	63	9.7 - 10.0	0.24	0.9738
Color preference index	63	0.71 - 0.82	0.41	0.8911

TABLE 8. Rotated factor pattern results of factor analysis for maximum thermal emittance temperature of 64 wall murals in Richmond, VA from 28 June 2018–19 July 2018. Factor analysis grouped parameters into factors from observed variables. Factor 1 indicates the strongest correlation. Factors 1-3 accounts for 81% of the variation in the data.

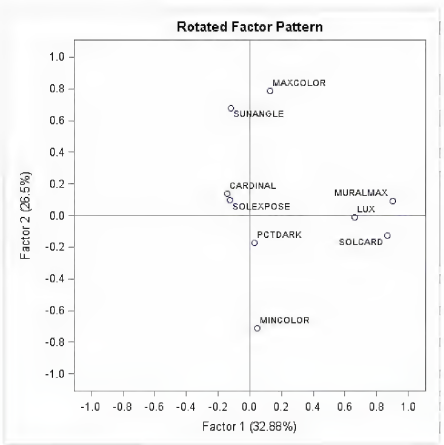

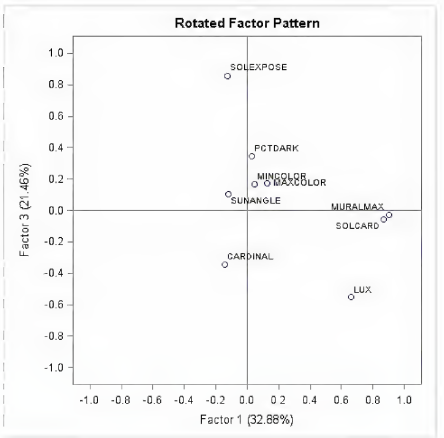

TABLE 9. Rotated factor pattern results of factor analysis for minimum thermal emittance temperature of 64 wall murals in Richmond, VA from 28 June 2018–19 July 2018. Factor analysis grouped parameters into factors from observed variables. Factor 1 indicates the strongest correlation. Factors 1-3 accounts for 81% of the variation in the data.

	Factor1	Factor2	Factor3	Factor4
Mural min. temp	0.84532	-0.05149	0.10702	-0.11827
Solar cardinal	0.80352	-0.07935	-0.20942	-0.05339
Max. color	0.11955	0.80279	0.14463	0.05796
Sun angle	-0.13526	0.67077	0.12866	-0.25069
Min. color	0.13533	-0.70394	0.18083	-0.10138
Solar exposure	-0.00528	0.09002	0.89185	0.06772
Lux	0.56676	0.01839	-0.65251	0.18449
% Dark	-0.01638	-0.16872	0.25812	0.77345
Cardinal	-0.11297	0.12307	-0.23994	0.69101

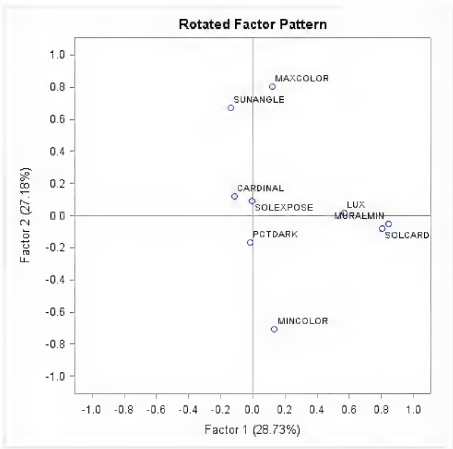

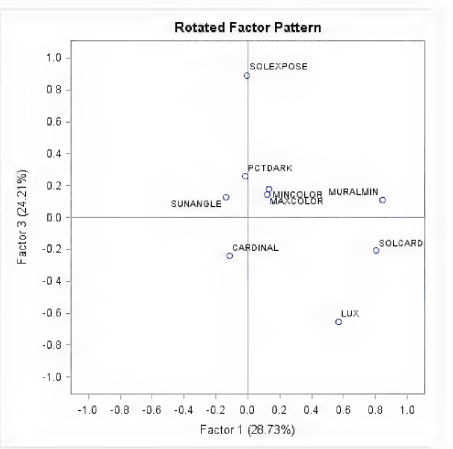

TABLE 10. Rotated factor pattern results of factor analysis for average thermal emittance temperature of 64 wall murals in Richmond, VA from 28 June 2018–19 July 2018. Factor analysis grouped parameters into factors from observed variables. Factor 1 indicates the strongest correlation. Factors 1-3 accounts for 81% of the variation in the data.

	Factor1	Factor2	Factor3	Factor4
Mural avg. temp.	0.89158	0.03080	0.03004	-0.08030
Solar cardinal	0.85102	-0.10626	-0.12065	-0.07783
Lux	0.61703	0.00157	-0.60033	0.17643
Max. color	0.12555	0.79326	0.16114	0.04592
Sun angle	-0.14521	0.67263	0.10534	-0.25302
Min. color	0.06667	-0.71153	0.15901	-0.10753
Solar exposure	-0.07007	0.09199	0.87896	0.05933
% Dark	0.02249	-0.17031	0.31219	0.76819
Cardinal	-0.14497	0.13497	-0.30895	0.69988

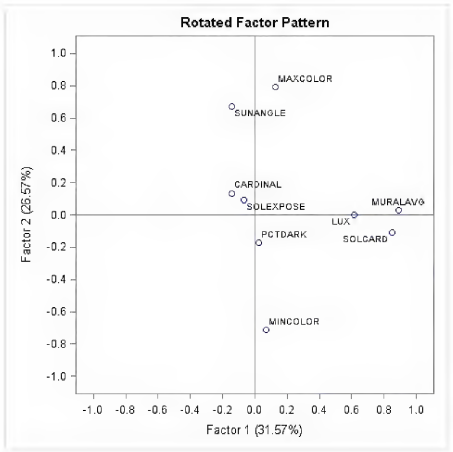

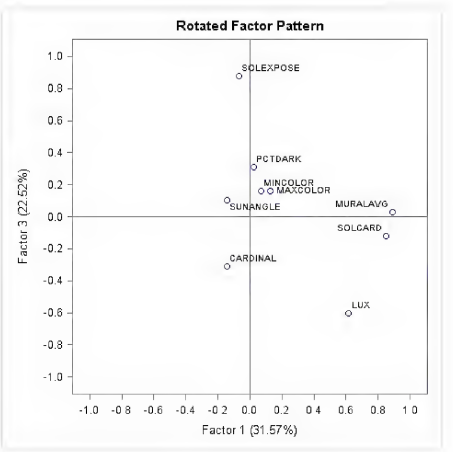

FIGURES

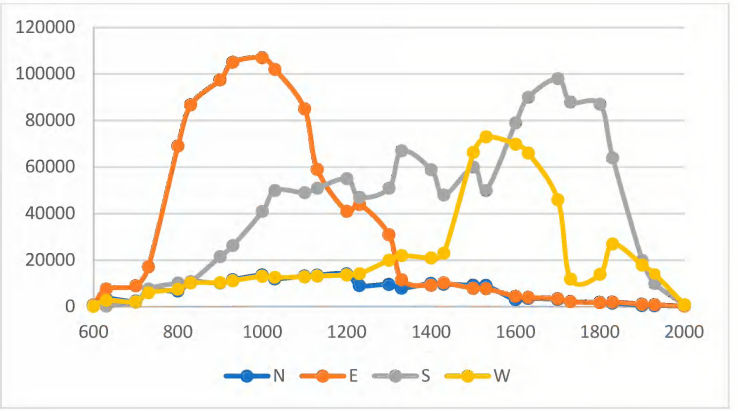

Figure 1. Lux readings of North, East, South, and West Cardinal points taken every 30 minutes in Richmond, Virginia from 6:00 to 20:00 EDT on 18 July 2018. Lux measurements recorded with AEMC model 1110 Light Meter Data Logger.

Figure 2. South wall art mural (A) and its corresponding thermal emittance image (B) indicating maximum, minimum, and average thermal emittance temperatures at 1305 hours EDT (Lux = 36000) 18 July, 2018. Maximum and minimum readings were taken within a fixed grid to control extraneous factors (e.g. windows, asphalt, skies) that would skew temperature readings.

Figure 3. North wall art mural (A) and its corresponding thermal emittance image (B) indicating maximum, minimum, and average thermal emittance temperatures at 1444 hours EDT (Lux = 9000), 09 July, 2018. Maximum and minimum readings were taken within a fixed grid to control extraneous factors (e.g. windows, asphalt, skies) that would skew temperature readings.

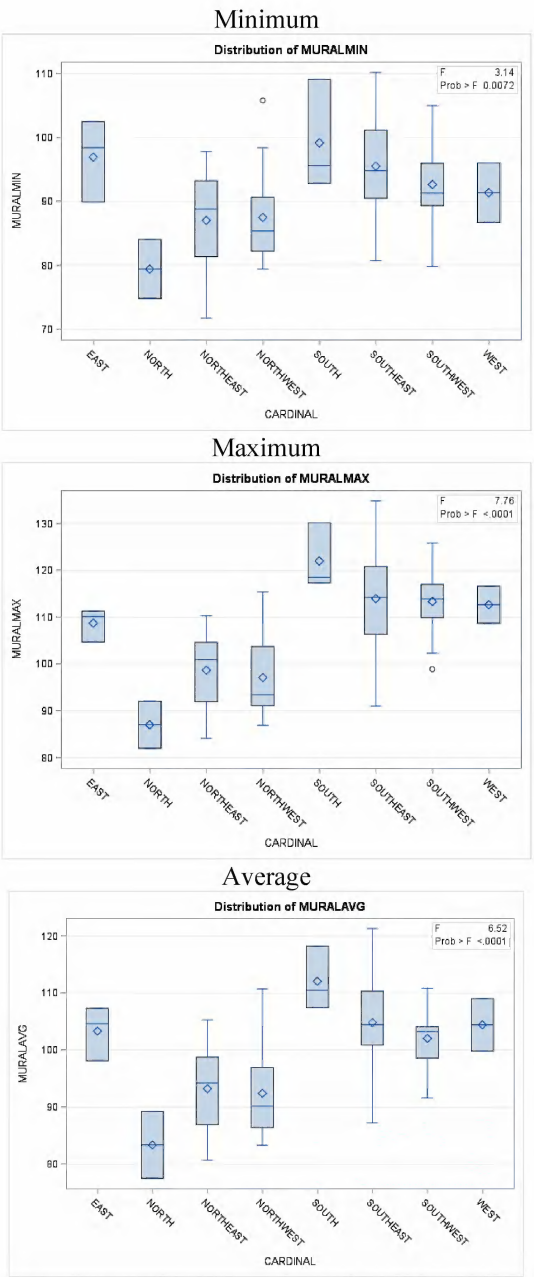

Figure 4. Minimum, maximum, and average thermal emittance (C) of wall murals by cardinal direction in Richmond, Virginia from 28 June 2018–19 July 2018 (n=64).

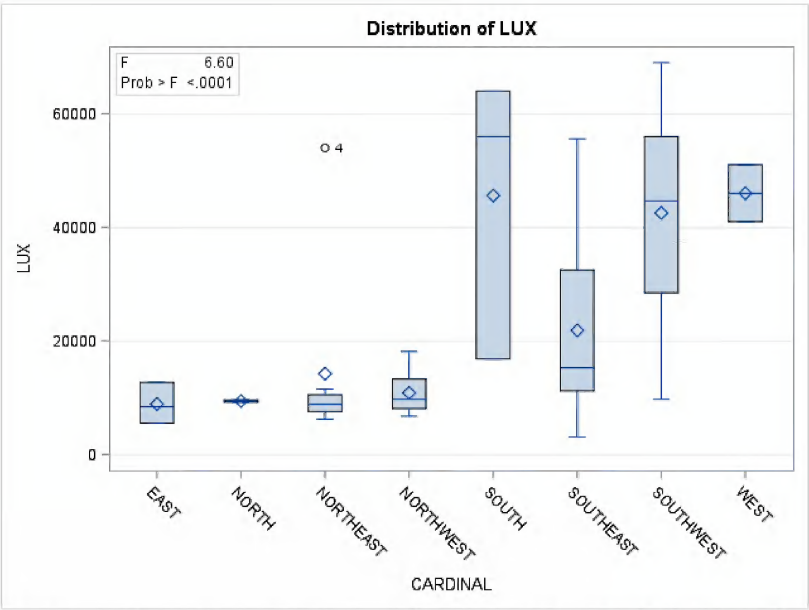

Figure 5. Average lux values of wall murals by cardinal direction in Richmond, Virginia from 28 June 2018 – 19 July 2018 (n=64).

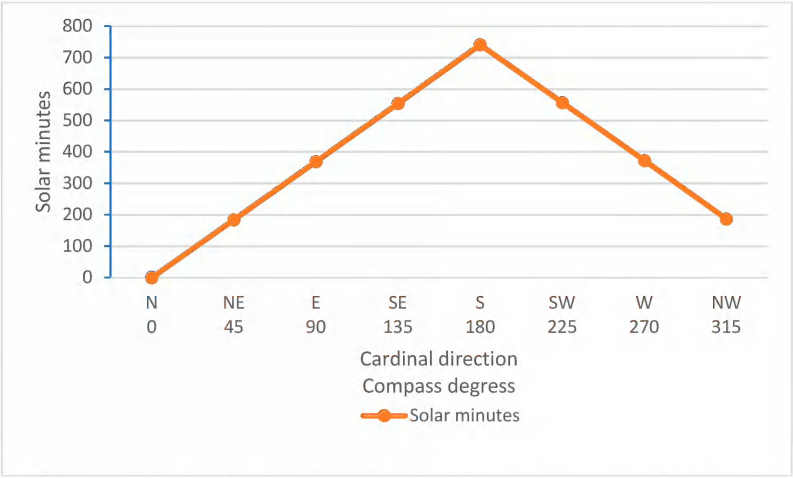

Figure 6. Solar minutes striking wall mural art per cardinal direction in Richmond, VA for June 2018.